

The Challenge of Being Straight: Explaining the Linearity of a Low-Spin $\{\text{FeNO}\}^7$ Unit in a Tropocoronand Complex

Espen Tangen,[†] Jeanet Conradie,[‡] and Abhik Ghosh^{*†}

Department of Chemistry, University of Tromsø, N-9037 Tromsø, Norway, and Department of Chemistry, University of the Free State, 9300 Bloemfontein, South Africa

Received May 15, 2005

We have carried out a density functional theory study of the $S = 1/2$ $\{\text{FeNO}\}^7$ tropocoronand complex, $\text{Fe}(5,5\text{-TC})\text{NO}$, as well as of some simplified models of this compound. The calculations accurately reproduce the experimentally observed trigonal-bipyramidal geometry of this complex, featuring a *linear* NO in an equatorial position and a very short Fe–N_{NO} distance. Despite these unique structural features, the qualitative features of the bonding turn out to be rather similar for $\text{Fe}(5,5\text{-TC})\text{NO}$ and $\{\text{FeNO}\}^7$ porphyrins. Thus, there is a close correspondence between the molecular orbitals (MOs) in the two cases. However, there is a critical, if somewhat subtle, difference in the nature of the singly occupied MOs (SOMOs) between the two. For square-pyramidal heme–NO complexes, the SOMO is primarily Fe d_{z^2} -based, which favors σ -bonding interactions with an NO π^* orbital, and hence a bent FeNO unit. However, for trigonal-bipyramidal $\text{Fe}(5,5\text{-TC})(\text{NO})$, the SOMO is best described as primarily Fe $d_{x^2-z^2}$ in character, with the Fe–N_{NO} vector being identified as the z direction. Apparently, such a d orbital is less adept at σ bonding with NO and, as such, π bonding dominates the Fe–NO interaction, leading to an essentially linear FeNO unit and a short Fe–N_{NO} distance.

Introduction

In view of their biological importance,^{1,2} metalloporphyrin–NO complexes have long served as the paradigms of transition metal–NO complexes in general.^{3–5} The geometric^{6–8} and electronic^{8–13} structures of these invariably low-spin complexes are reasonably well-understood and may

be conveniently summarized in terms of the so-called Enemark–Feltham electron counts (n),^{14,15} defined as the number of metal d electrons plus NO π^* electrons. Thus, for $n = 6$, as in the case of Mn(II)–NO and Fe(III)–NO porphyrins, the MNO unit is generally approximately linear because this maximizes metal(d_{π})–NO(π^*) π bonding.^{3,16,17} However, for $n = 7$ and 8, as in the case of Fe(II)–NO and Co(II)–NO porphyrins, respectively, the MNO unit is strongly bent and the highest occupied molecular orbital (HOMO) may be viewed as a σ -type interaction between the metal d_{z^2} orbital and an NO π^* orbital.⁹

Non-heme transition metal–NO centers exhibit a broader range of geometric and electronic structures.^{4,5} Thus, a number of non-heme $\{\text{FeNO}\}^7$ complexes (with the superscript referring to the Enemark–Feltham electron count)

* To whom correspondence should be addressed. E-mail: abhik@chem.uit.no.

[†] University of Tromsø.

[‡] University of the Free State.

- (1) Ignarro, L. J. In *Nitric Oxide: Biology and Pathobiology*; Ignarro, L., Ed.; Academic Press: San Diego, 2000; pp 3–19.
- (2) Boon, E. M.; Marletta, M. A. *J. Inorg. Biochem.* **2005**, *99*, 892–902.
- (3) Wyllie, G. R. A.; Scheidt, W. R. *Chem. Rev.* **2002**, *102*, 1067–1089.
- (4) Hayton, T. W.; Legzdins, P.; Sharp, W. B. *Chem. Rev.* **2002**, *102*, 935–991.
- (5) McCleverty, J. A. *Chem. Rev.* **2004**, *104*, 403–418.
- (6) Ellison, M. K.; Scheidt, W. R. *J. Am. Chem. Soc.* **1997**, *119*, 7404–7405.
- (7) Scheidt, W. R.; Duval, H. F.; Neal, T. J.; Ellison, M. K. *J. Am. Chem. Soc.* **2000**, *122*, 4651–4659.
- (8) Wyllie, G. R. A.; Schulz, C. E.; Scheidt, W. R. *Inorg. Chem.* **2003**, *42*, 5722–5734.
- (9) Wondimagegn, T.; Ghosh, A. *J. Am. Chem. Soc.* **2000**, *122*, 8101–8102.
- (10) Hayes, R. G.; Ellison, M.; Scheidt, W. R. *Inorg. Chem.* **2000**, *39*, 3665–3668.
- (11) Wondimagegn, T.; Ghosh, A. *J. Am. Chem. Soc.* **2001**, *123*, 5680–5683.

(12) Zhang, Y.; Mao, J.; Godbout, N.; Oldfield, E. *J. Am. Chem. Soc.* **2002**, *124*, 13921.

(13) Ghosh, A. *Acc. Chem. Res.* **2005**, in press.

(14) Enemark, J. H.; Feltham, R. D. *Coord. Chem. Rev.* **1974**, *13*, 339–406.

(15) For a review, see: Westcott, B. L.; Enemark, J. L. In *Inorganic Electronic Structure and Spectroscopy*; Solomon, E. I., Lever, A. B. P., Eds.; Wiley: New York, 1999; Vol. 2, pp 403–450.

(16) Walker, F. A. *J. Inorg. Biochem.* **2005**, *216*, 235.

(17) Patra, A. K.; Rose, M. J.; Olmstead, M. M.; Mascharak, P. K. *J. Am. Chem. Soc.* **2004**, *126*, 4780–4781.

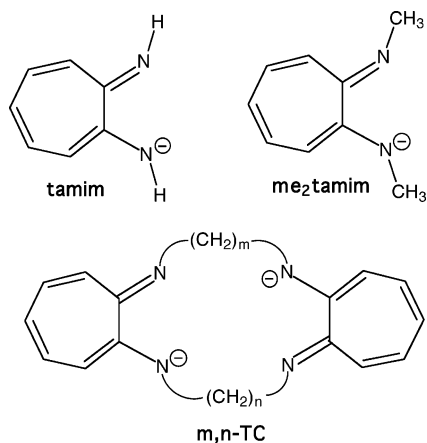


Figure 1. Tropocoronand ligands, $[m,n\text{-TC}]^{2-}$. Also shown are the tamim and me_2tamim ligands.

exhibit $S = 3/2$ ground states, arising from antiferromagnetic coupling between $S = 5/2$ Fe(III) centers and $S = 1$ NO⁻ units.¹⁸ However, Franz and Lippard have described an unusual $S = 1/2$ five-coordinate $\{\text{FeNO}\}^7$ complex based on a macrocyclic tetradentate tropocoronand ligand;¹⁹ the complex exhibits a trigonal-bipyramidal geometry with an essentially *linear*, equatorial (as opposed to axial or apical) NO. Experimentally, this complex has been rigorously characterized, but a molecular orbital (MO) description of the bonding has yet to be given. Specifically, does the unique linear $\{\text{FeNO}\}^7$ unit imply a radically different electronic structure relative to heme-NO complexes and, if so, how? This is the key question that we sought to explore in this study.

In a certain sense, tropocoronand ligands ($m,n\text{-TC}^{2-}$; see Figure 1) are rather similar to porphyrins. Thus, for the dianionic ligands, each TC nitrogen carries a formal charge of $-1/2$, as in a porphyrin. However, depending on the lengths of the polymethylene tethers, TC ligands might impose significantly different steric constraints on the metal ions they coordinate, compared to a porphyrin. Geometrical differences between TCs and porphyrins necessarily engender key

differences in the electronic structure and coordination geometry between the two families of complexes, and we will attempt to present a theoretical analysis of these differences for $\{\text{FeNO}\}^7$ derivatives. A theoretical approach also readily permits us to simplify a TC ligand to a pair of tropamiminato (tamim, named by analogy with tropolonato) or N,N' -dimethyltropamiminato (me_2tamim) ligands, which are shown in Figure 1. We will see that these simpler ligands allow us to transcend some of the geometrical constraints of the macrocyclic TC ligands and to examine the relative stabilities of different five-coordinate stereochemistries of model $\{\text{FeNO}\}^7$ complexes. Thus, a second goal of this study has been to obtain a sense of the “inherent” stereochemical preferences of low-spin five-coordinate $\{\text{FeNO}\}^7$ complexes.

Details of the Calculations

Using the ADF 2004 program system, we carried out density functional theory (DFT; PW91/STO-TZP)²⁰ calculations on the following complexes: $\text{Fe}(\text{tamim})_2\text{NO}$, $\text{Fe}(\text{me}_2\text{tamim})_2\text{NO}$, and $\text{Fe}(\text{5,5-TC})\text{NO}$. For each complex, we considered square-pyramidal (SQP) and trigonal-bipyramidal (TBP) geometries as well as $S = 1/2$ and $3/2$ electronic states. For the TBP complexes, both axial (TBP_{ax}) and equatorial (TBP_{eq}) NO orientations were considered. Judicious use of symmetry constraints allowed us to obtain optimized geometries for the different stereochemistries of interest. In addition, fully unconstrained geometry optimizations were also carried out for each molecule. Table 1 summarizes highlights of the calculated energetics, structural, and spin population data. Figures 2–5 present highlights of the optimized structures as well as the spin-density profiles for the various species studied (albeit only for the $S = 1/2$ states), while Figure 6 depicts selected MOs for $\text{Fe}(\text{tamim})_2\text{NO}$.

Results and Discussion

Table 1 shows that an $S = 1/2$ spin state is favored for all of the molecules studied, consistent with experiment as well as with our intuitive notion of the strongly electron-donating nature of the ligands. Given the high energies of the $S = 3/2$ states, we will not discuss them further in this paper. Our other main findings are as follows.

Table 1. Relative Energetics, FeNO Geometry Parameters, and FeNO Atomic Spin Populations (s) for the Various Species Studied

compound	symmetry			E_{rel} (eV)	distances and angles (Å and deg)			Mulliken spin populations		
	spin	geometry	symmetry		$d(\text{FeN}_{\text{NO}})$	$d(\text{NO})$	$\angle\text{FeNO}$	s_{Fe}	s_{N}	s_{O}
$\text{Fe}(\text{tamim})_2\text{NO}$	$1/2$	SQP	C_1	0.000	1.692	1.193	145.6	0.8429	0.0250	-0.0112
	$1/2$	TBP _{eq}	C_2	0.091	1.656	1.188	180.0	0.9308	-0.0740	-0.0734
	$1/2$	TBP _{ax}	C_s	0.643	1.638	1.183	172.5	0.9429	-0.1221	-0.0875
	$1/2$	SQP	C_s	0.029	1.685	1.194	147.2	0.8506	0.0336	-0.0098
$\text{Fe}(\text{tamim})_2\text{NO}$	$3/2$	TBP _{eq}	C_1	0.957	1.728	1.188	152.2	3.1402	-0.3587	-0.285
	$3/2$	TBP _{eq}	C_2	0.974	1.719	1.183	180.0	3.2224	-0.4293	-0.3254
	$3/2$	TBP _{ax}	C_s	0.962	1.775	1.201	136.0	2.7820	-0.0802	-0.0941
	$3/2$	SQP	C_s	1.248	1.972	1.207	138.9	1.6836	0.7086	0.3583
$\text{Fe}(\text{me}_2\text{tamim})_2\text{NO}$	$1/2$	TBP _{eq}	C_1	0.000	1.655	1.192	167.2	0.9480	-0.0740	-0.0706
	$1/2$	TBP _{eq}	C_2	0.010	1.651	1.191	180.0	0.9632	-0.0912	-0.0809
	$1/2$	TBP _{ax}	C_s	0.475	1.634	1.185	178.5	0.9720	-0.1204	-0.0884
	$1/2$	SQP	C_s	0.352	1.686	1.199	144.0	0.9655	0.0013	-0.0316
$\text{Fe}(\text{me}_2\text{tamim})_2\text{NO}$	$3/2$	TBP _{ax}	C_1	0.745	1.741	1.196	142.5	2.6496	-0.0224	-0.0471
	$3/2$	TBP _{eq}	C_2	0.897	1.722	1.186	180.0	3.2154	-0.4392	-0.3287
	$3/2$	TBP _{ax}	C_s	0.967	1.755	1.199	146.2	2.6498	0.0085	-0.0518
	$3/2$	SQP	C_s	1.122	1.720	1.189	151.6	3.1647	-0.3707	-0.2923
$\text{Fe}(\text{5,5-TC})_2\text{NO}$	$1/2$	TBP _{eq}	C_1	0.000	1.649	1.194	178.5	0.9941	-0.1059	-0.0854
	$1/2$	SQP	C_s	1.287	1.686	1.192	144.9	0.9486	0.0131	-0.0256
	$3/2$	TBP _{eq}	C_1	0.805	1.727	1.202	148.0	2.7322	-0.0836	-0.0911
	$3/2$	SQP	C_s	1.911	1.729	1.184	151.1	3.2308	-0.3581	-0.2891

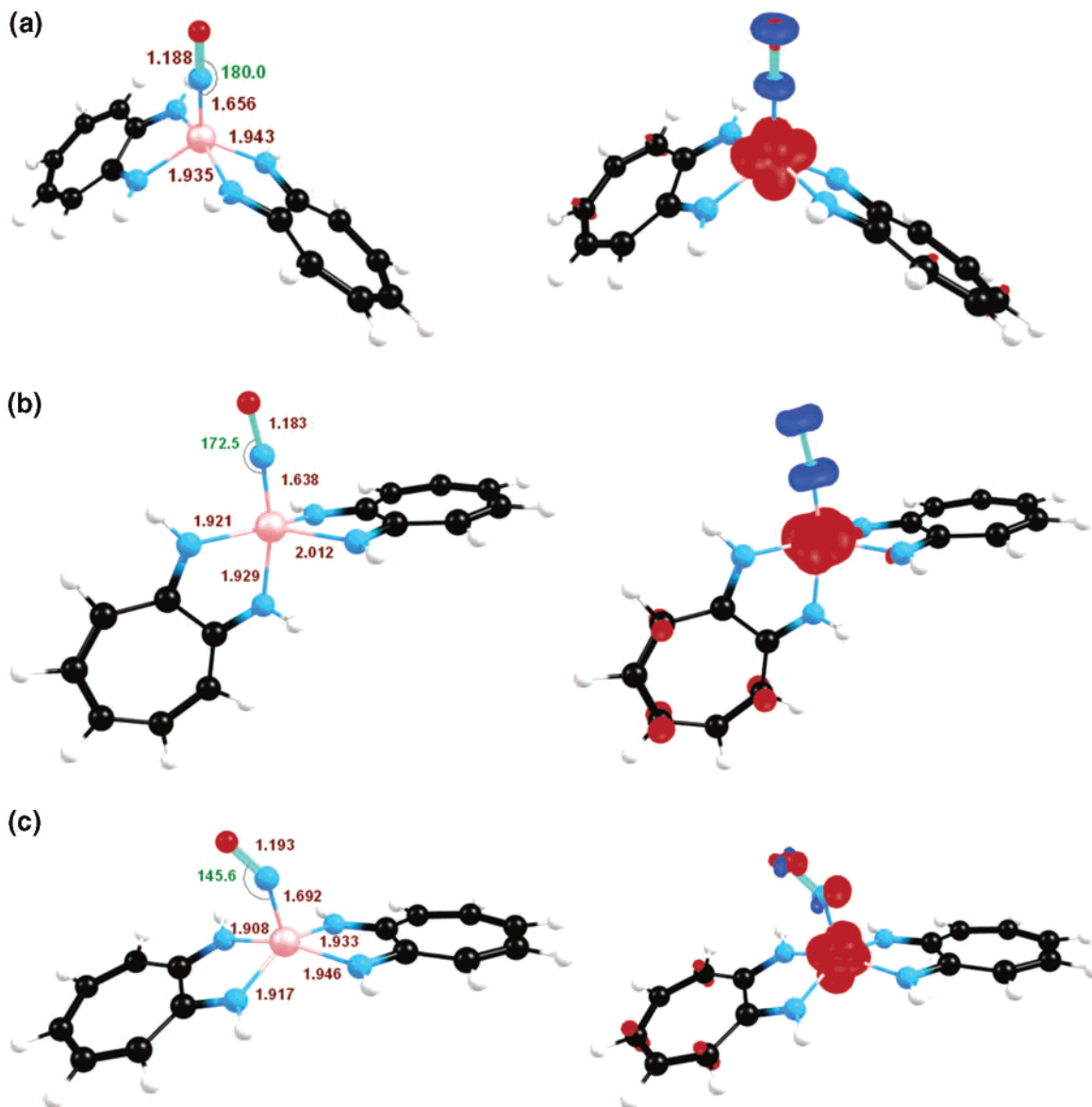


Figure 2. Structural highlights (angstroms in brown and degrees in green) and spin-density plots for different conformations of $Fe(tamim)_2(NO)$: (a) TBP_{eq} (C_2), (b) TBP_{ax} (C_s), and (c) SQP (C_1). Majority and minority spins are indicated in red and blue, respectively.

(a) Energetics of Different Coordination Geometries.

For $Fe(tamim)_2NO$, the lowest-energy conformation corresponds to SQP coordination, with the TBP_{eq} geometry only about 0.1 eV higher in energy, while the TBP_{ax} geometry is significantly higher in energy. In contrast, for $Fe(me_2-tamim)_2NO$, the TBP_{eq} geometry is clearly the lowest-energy conformation, with the SQP geometry 0.35 eV higher and the TBP_{ax} form still higher in energy. The results for $Fe(5,5-TC)NO$ are qualitatively similar to those for $Fe(me_2-tamim)_2NO$: the TBP_{eq} geometry has the lowest energy, the SQP geometry is nearly 0.9 eV higher in energy, and the

TBP_{ax} form is higher still. The fact that the TBP_{eq} geometry is substantially favored over the TBP_{ax} geometry was also noted in some of the early theoretical studies on transition-metal nitrosyls.^{14,21} Nonetheless, we will again rationalize this finding in terms of the MO picture obtained here. Another interesting issue is the reversal of stereochemical preference between $Fe(tamim)_2NO$, on the one hand, and $Fe(me_2-tamim)_2NO$ and $Fe(5,5-TC)NO$, on the other hand. In other words, why does N alkylation of the tamim ligands, whether with methyl groups or with the polymethylene tethers of the 5,5-TC ligand, tip the stereochemical preference from SQP to TBP_{eq} ? Is this an electronic effect?

(b) MO Descriptions. Figure 6 depicts selected majority-spin-occupied MOs of the low-spin SQP, TBP_{eq} , and TBP_{ax} forms of $Fe(tamim)_2NO$ as well as the lowest unoccupied MOs (LUMOs) of each molecule. For all of the molecules,

(18) Brown, C. A.; Pavlosky, M. A.; Westre, T. E.; Zhang, Y.; Hedman, B.; Hodgson, K. O.; Solomon, E. I. *J. Am. Chem. Soc.* **1995**, *117*, 715–732.

(19) Franz, K. J.; Lippard, S. J. *J. Am. Chem. Soc.* **1999**, *121*, 10504–10512.

(20) All calculations were carried out using the ADF 2004 program system, using methods described in: Velde, G. T.; Bickelhaupt, F. M.; Baerends, E. J.; Guerra, C. F.; van Gisbergen, S. J. A.; Snijders, J. G.; Ziegler, T. *J. Comput. Chem.* **2001**, *22*, 931–967.

(21) Hoffmann, R.; Chen, M. M. L.; Elian, M.; Rossi, A. R.; Mingos, D. M. P. *Inorg. Chem.* **1974**, *13*, 2666–2675.

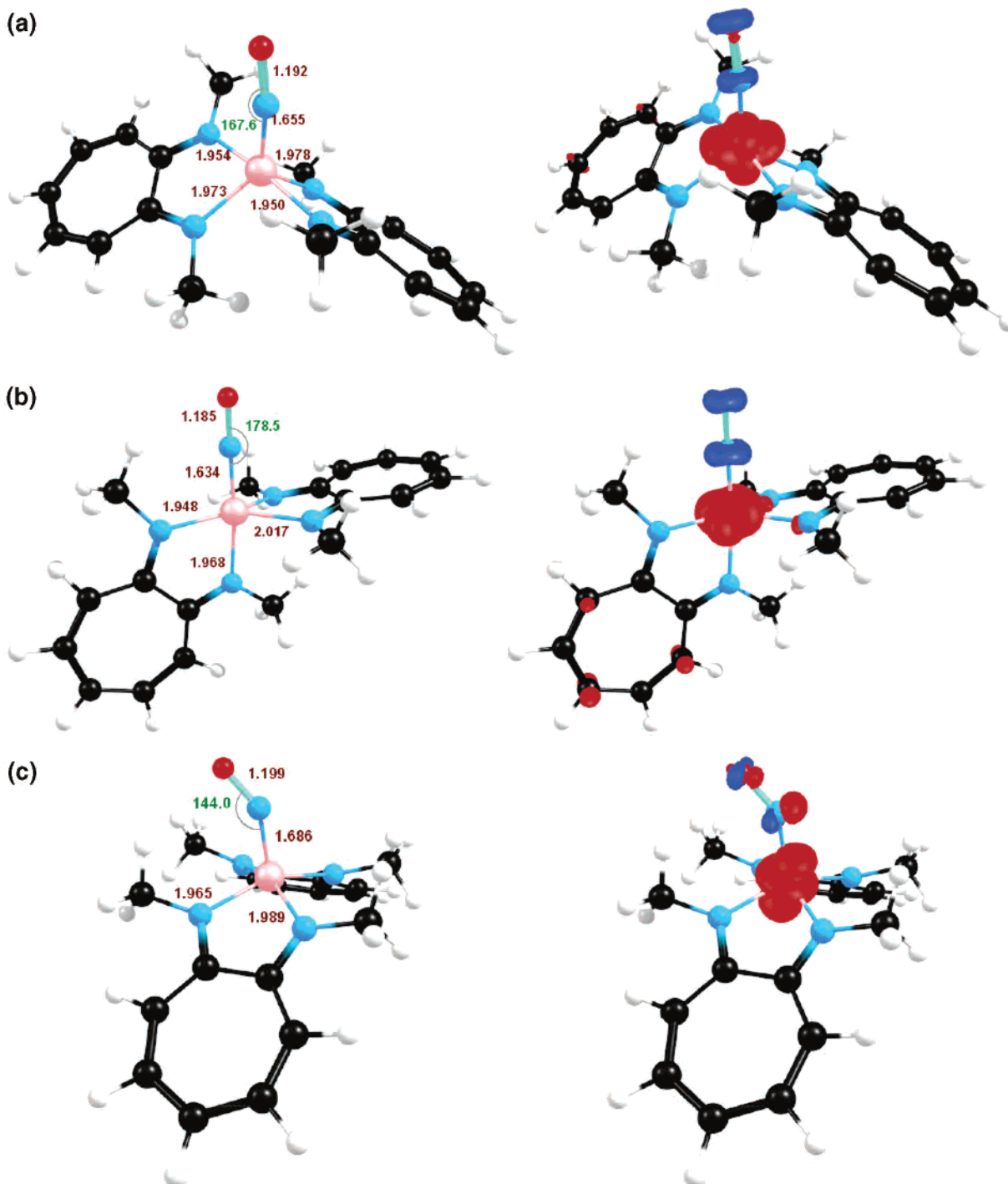


Figure 3. Structural highlights (angstroms in brown and degrees in green) and spin-density plots for different conformations of $\text{Fe}(\text{me}_2\text{tamim})_2(\text{NO})$: (a) TBP_{eq} (C_2), (b) TBP_{ax} (C_s), and (c) SQP (C_1). Majority and minority spins are indicated in red and blue, respectively.

each majority-spin MO also has a rather similar-looking minority-spin MO partner. Note that certain of the metal d orbitals contribute significantly to several canonical MOs; moreover, several of the MOs involve considerable metal–ligand orbital mixing. Both these factors make it somewhat difficult to describe the electronic structures in simple ligand field theory terms. Nonetheless, two factors contributing to the instability of the TBP_{ax} geometries are readily discerned. First, note that for the SQP and TBP_{eq} geometries, none of the higher occupied MOs exhibits significant metal–ligand antibonding interactions, whereas in the TBP_{ax} case, the α

HOMO (which may be viewed as the SOMO, the “singly” occupied MO) as well as the α HOMO-2 and β HOMO-1 all exhibit significant metal–tamim σ -antibonding character. Second, and perhaps more importantly, the metal–tamim bonding interactions are stronger in the SQP and TBP_{eq} cases than in the TBP_{ax} case. Thus, note the strong metal–tamim bonding interaction in the majority-spin HOMO-19 in the SQP and TBP_{eq} cases in Figure 6 (at the top of the figure); there is no comparable orbital interaction in the TBP_{ax} case.

For the TBP_{eq} stereochemistry of $\text{Fe}(\text{tamim})_2\text{NO}$ and for $\text{Fe}(5,5\text{-TC})$, the electronic configuration of the metal may

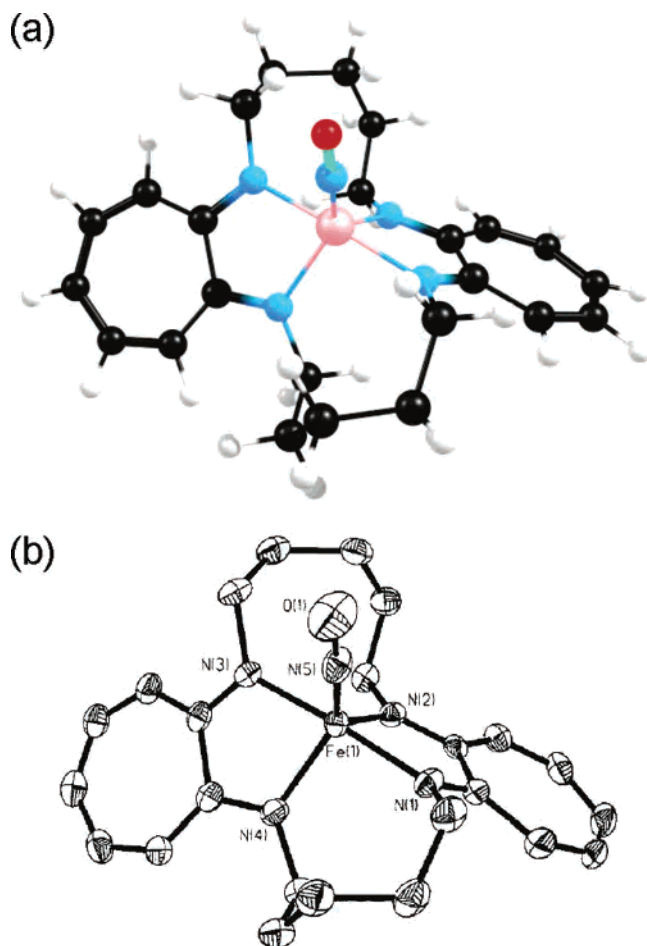


Figure 4. Qualitative comparison of the (a) optimized and (b) crystallographic structures of Fe(5,5-TC)(NO). Majority and minority spins are indicated in red and blue, respectively.

be described as $(d_{xz}, d_{yz})^4 d_{xy}^2 d_{x^2-z^2}^1$, where the seven electrons correspond to the Enemark–Feltham electron count in question and the z direction corresponds to the Fe–N_{NO} axis. The Fe d_{π} orbitals (d_{xz} and d_{yz}) are readily discernible in Figure 6. The majority-spin HOMO-2 may be viewed as an Fe d_{xy} -based MO. Interestingly, the “SOMO” (i.e., the occupied majority-spin MO that does not have an occupied minority-spin partner) is actually best described as a $d_{x^2-z^2}$ orbital rather than as primarily d_{z^2} , as in a heme–NO complex. This may also be seen from the spin-density profiles of the various TBP_{eq} species shown in Figures 2, 3, and 5. The reason for this is that, in the TBP_{eq} case, the strongest ligand field is clearly along the pseudo-3-fold axis of the trigonal bipyramid (which we may call the y axis), resulting from a pair of tropocoronand nitrogens. Thus, in a ligand field theory picture, the unoccupied d orbital may be described as d_{y^2} .

Compared with the SQP case, where there is a small but significant amount of majority spin on the NO moiety (which is consistent with the observation of NO nitrogen hyperfine coupling in the EPR spectra of heme–NO complexes), Table 1 and Figures 2, 3, and 5 show that there is actually a small amount of minority spin on the NO unit in the TBP_{eq} complexes. This minority-spin density arises from a small offset between the majority- and minority-spin Fe(d_{π})–NO-

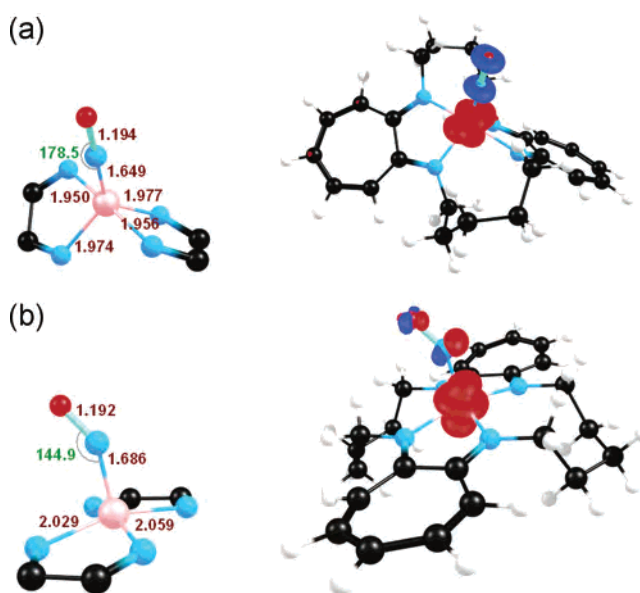


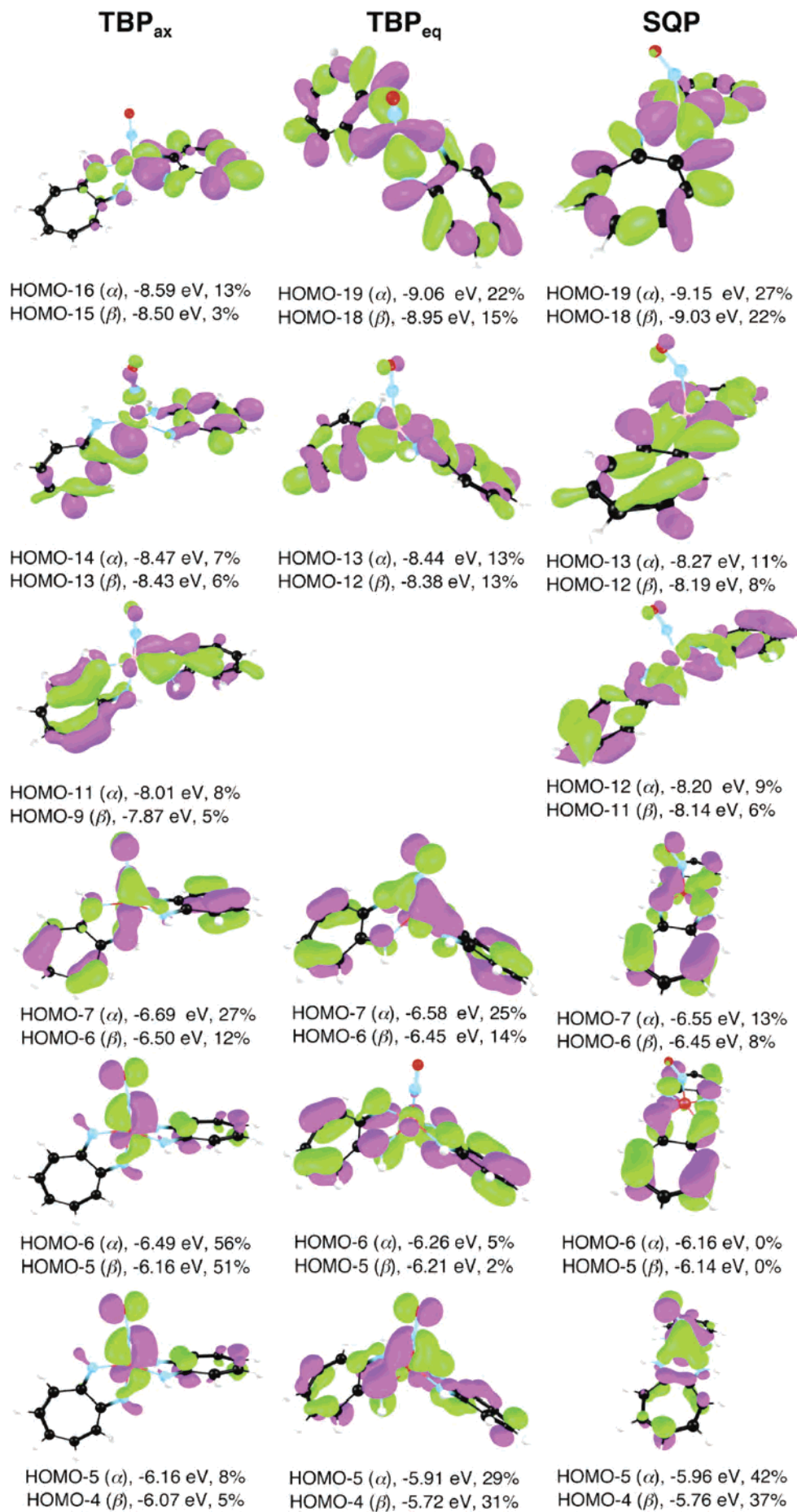
Figure 5. Structural highlights (angstroms in brown and degrees in green) and spin-density profiles for the (a) TBP_{eq} (C₁) and (b) SQP (C₂) conformations of Fe(5,5-TC)(NO).

(π^*) π MOs. This aspect of the spin-density profile is consistent with Franz and Lippard’s description¹⁹ of the $\{\text{FeNO}\}^7$ center in Fe(5,5-TC)NO as a low-spin $S = 1/2$ Fe(III) strongly antiferromagnetically coupled to an $S = 1$ NO[−] group, as discussed further below.

(c) Molecular Structures. We will pay attention to the following questions as we discuss the various optimized geometries. First, how do the different stereochemistries vary with respect to bond distances and angles? Second, how do the optimized structures compare with relevant experimental results? Third, are the various optimized structures qualitatively consistent with the MO picture presented above?

Let us first consider the calculated Fe–N distances involving the tamim fragments. Note that two of the three equatorial Fe–N vectors in the TBP_{ax} structures are unusually long (>2.00 Å) compared with all other Fe–N distances in this study. These two distances reflect the metal–tamim antibonding interactions in the HOMO (SOMO) of all of the TBP_{ax} species (see Figure 6). Otherwise, the Fe–N distances involving the tamim fragments are relatively short, as expected for low-spin Fe(III) centers: 1.91–1.95 Å for SQP Fe(tamim)₂NO (Figure 2), 1.93–1.94 Å for TBP_{eq} Fe(tamim)₂NO (Figure 2), and 1.95–1.98 Å for TBP_{eq} Fe(5,5-TC)NO.

Regarding the FeNO units, the calculated Fe–N_{NO} distances are considerably shorter in the TBP_{eq} structures than in the SQP ones. Thus, the Fe–N_{NO} distance is only 1.656 Å in the TBP_{eq} conformation of Fe(tamim)₂NO, a full 0.046 Å shorter than the distance of 1.692 Å for the TBP_{ax} conformation. In a similar vein, the calculated Fe–N_{NO} distance in Fe(5,5-TC)NO is 1.649 Å, which is considerably shorter than that for heme–NO model compounds Fe(P)(NO) (1.704 Å) and Fe(P)(ImH)(NO) (1.741 Å), where P refers to porphine and ImH to imidazole. These calculated differences nicely mirror experimental results. Thus, experimentally, the Fe–N_{NO} distance in Fe(5,5-TC)NO is 1.670(4) Å,



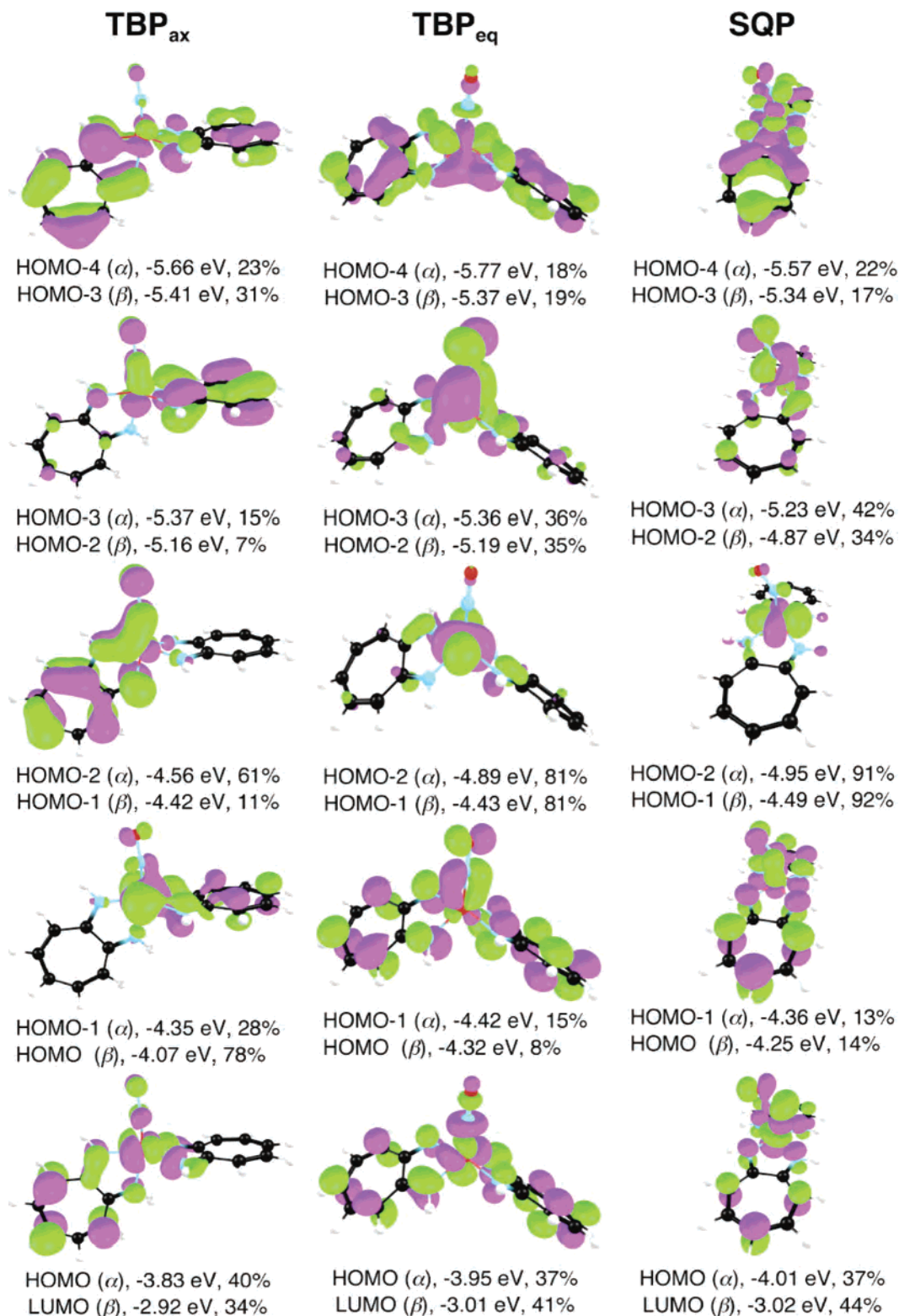


Figure 6. Selected higher energy occupied MOs and the LUMOs of different conformations of $Fe(tamim)_2(NO)$. For every majority-spin (α) MO, a qualitatively similar-looking minority-spin (β) MO was also identified. Percent iron contributions are indicated.

compared to 1.717(7) Å for $Fe(TPP)(NO)$ (TPP = tetraphenylporphyrin).

Interestingly, the calculated NO distance varies much less between the TBP_{eq} and SQP stereochemistries: for $Fe(tamim)_2NO$, the NO distances are 1.188 and 1.193 Å, respectively, in the two conformations, thus differing by only 0.005 Å. This may be viewed as qualitatively consis-

tent with very similar NO stretching frequencies observed for $Fe(5,5-TC)NO$ (1692 cm^{-1}) and $Fe(TPP)(NO)$ (1670 cm^{-1}).

A comment is also in order on the three-dimensional conformation of $Fe(5,5-TC)NO$. Thus, Figure 4 shows that a DFT geometry optimization accurately reproduces the experimentally observed conformation for this molecule.

Last but not least is the Fe–N–O angle. Why is the FeNO unit strongly bent (the angle being about 145°) in the SQP structures, while it is essentially linear for TBP_{eq} conformations? This may seem especially surprising, considering the geometrical similarity of the SQP and TBP_{eq} conformations. Thus, starting with the SQP conformation of Fe(tamim)₂NO, we can obtain the TBP_{eq} conformation by simply twisting the equatorial chelate rings in opposite directions. Indeed, a careful examination of Figure 6 shows that there is a close similarity between nearly *all* of the higher occupied MOs of the two conformations. Thus, the very different Fe–N–O angles must result from relatively subtle differences in orbital interactions between the SQP and TBP_{eq} conformations.

To identify these subtle differences, we decided to compare the MO energies for Fe(5,5-TC)(NO) (TBP_{eq}) as well as for Fe(P)(NO) as a function of the Fe–N–O angle (in a Walsh diagram-type approach), all other internal coordinates being fully optimized. The results of these studies (not explicitly shown) indicated that while the Fe–N–O angle favors Fe–N–O σ bonding (i.e., lowers the energy of the d_{z^2} or $d_{x^2-z^2}$ -based MO), it raises the energies for Fe(d_{xy})–NO(π^*) bonding MOs. As a result of these two opposing effects, the net energetic cost of FeNO deformation is remarkably small. Thus, an TBP_{eq} Fe(5,5-TC)(NO) structure with an Fe–N–O angle constrained to 140°, but otherwise fully optimized, is only about 0.1 eV higher than the global minimum (which has a near-linear Fe–N–O angle). In the same spirit, a C_{4v} structure of nitrosylheme (with a perfectly upright NO group) was found to be only 0.2 eV higher than the C_s global minimum with an Fe–N–O angle of 142°; qualitatively similar energies have also been obtained for nitrosylhemes by other researchers.^{22–24} In other words, both cases are characterized by a shallow Fe–N–O bending potential curve. Yet, in one case [Fe(5,5-TC)(NO)], Fe–NO π bonding wins out, leading to a linear FeNO unit, whereas in the other case [Fe(P)(NO)], Fe–NO σ bonding gains the upper hand, leading to a bent FeNO unit. What accounts for the difference? Having carefully eliminated other factors, we conclude that the nature of the SOMO is the key determinant of the Fe–N–O angle: the primarily d_{z^2} -based SOMO for SQP species such as Fe(P)(NO) is simply more conducive to Fe(d)–NO(π^*) σ bonding than the $d_{x^2-z^2}$ -like SOMO of the TBP_{eq} Fe(5,5-TC)(NO). As a result, the Fe–NO bonding in the latter case is nearly pure π in character.

Conclusion

Time was when bent metal–NO units demanded theoretical explanations.^{14,15,21} Franz and Lippard's synthesis of a

low-spin {FeNO}⁷ complex with a near-linear FeNO unit turned the tables on this question, posing a new theoretical challenge, which we took on in this study. Looking back at our findings, the linear FeNO unit in Fe(5,5-TC)(NO) seems to have been somewhat of a red herring, suggesting, as it did to us and presumably to others as well, a radically different electronic structure relative to SQP heme–NO derivatives. Instead, one of our key findings is that the bonding in the SQP and TBP_{eq} stereochemistries is not *qualitatively* different. Thus, in general, there is a close correspondence between the MOs in the two cases. However, there is a critical, if somewhat subtle, difference in the nature of the SOMOs between the two geometries. In the SQP case (such as heme–NO complexes), the SOMO is primarily Fe d_{z^2} -based, which favors σ -bonding interactions with an NO π^* orbital, and hence a bent FeNO unit. However, in the TBP_{eq} case [such as for Fe(5,5-TC)(NO)], the SOMO is best described as primarily Fe $d_{x^2-z^2}$ in character. Presumably, such a d orbital is less suitable for σ bonding with NO and, as such, π bonding dominates the Fe–N–O interaction, leading to an essentially linear FeNO unit. Overall, the fact that our calculations accurately reproduce the unique, experimentally observed structure of Fe(5,5-TC)(NO) is strong evidence that we have also obtained a correct electronic–structural description for this species.

We have also obtained a “feel” for the relative stabilities for different alternative geometries for low-spin {FeNO}⁷ complexes. For the sterically unhindered model compound Fe(tamim)₂NO, the SQP and TBP_{eq} stereochemistries are nearly equienergetic, with the former very slightly lower in energy. Steric constraints, such as those operating for Fe(5,5-TC)(NO), can readily reverse this stereochemical preference. In contrast, the TBP_{ax} geometry is strongly disfavored on electronic grounds, namely, stronger metal–ligand bonding interactions for the SQP and TBP_{eq} stereochemistries and stronger metal–ligand antibonding interactions for TBP_{ax}.

Equipped with these insights, we look forward to exploring additional non-heme–NO complexes, including other tropocoronand NO complexes reported by Lippard and co-workers.^{25,26}

Acknowledgment. This work was supported by the Research Councils of Norway and of South Africa.

Supporting Information Available: Optimized Cartesian coordinates. This material is available free of charge via the Internet at <http://pubs.acs.org>.

IC050781A

(22) Rovira, C.; Kunc, K.; Hutter, J.; Ballone, P.; Parrinello, M. *J. Phys. Chem. A* **1997**, *101*, 8914–8925.

(23) Patchkovskii, S.; Ziegler, T. *J. Phys. Chem. A* **1997**, *101*, 8914–8925.

(24) Zemojtel, T.; Rini, M.; Heyne, K.; Dandekar, T.; Nibbering, E. T. J.; Kozłowski, P. M. *J. Am. Chem. Soc.* **2004**, *126*, 1930–1931.

(25) Franz, K. J.; Lippard, S. J. *J. Am. Chem. Soc.* **1998**, *120*, 9034–9040.

(26) Franz, K. J.; Doerrer, L. H.; Spingler, B.; Lippard, S. J. *Inorg. Chem.* **2001**, *40*, 9034–9040.